Continued Development of a Global Heat Transfer Measurement System at AEDC Hypervelocity Wind Tunnel 9

Inna Kurits* & M. J. Lewis†
Department of Aerospace Engineering
University of Maryland
College Park, MD 20742

M. P. Hamner‡
LeaTech LLC
Frederick, MD 21701

Joseph D. Norris§
Aerospace Testing Alliance
Arnold Engineering Development Center - White Oak
Silver Spring, Maryland 20903-1005

Heat transfer rates are an extremely important consideration in the design of hypersonic vehicles such as atmospheric reentry vehicles. This paper describes the development of a data reduction methodology to evaluate global heat transfer rates using surface temperature-time histories measured with the temperature sensitive paint (TSP) system at AEDC Hypervelocity Wind Tunnel 9. As a part of this development effort, a scale model of the NASA Crew Exploration Vehicle (CEV) was painted with TSP and multiple sequences of high resolution images were acquired during a five-run test program. Heat transfer calculation from TSP data in Tunnel 9 is challenging due to relatively long run times, high Reynolds number environment and the desire to utilize typical stainless steel wind tunnel models used for force and moment testing. An approach to reduce TSP data into convective heat flux was developed, taking into consideration the conditions listed above. Surface temperatures from high quality quantitative global temperature maps acquired with the TSP system were then used as an input into the algorithm. Preliminary comparison of the heat flux calculated using the TSP surface temperature data with the value calculated using the standard thermocouple data is reported.

Nomenclature

ANSYS	=	finite element modeling tool for structural and thermal analysis
CCD	=	charge coupled device
CEV	=	Crew Exploration Vehicle
cp	=	specific heat of nitrogen at constant pressure, 0.2481 BTU/lbm-°R
C_p	=	specific heat
deg, °	=	degree, angular
F	=	degree, Fahrenheit
ft	=	feet
H_o	=	calculated total enthalpy, BTU/lbm
Hz	=	Hertz
in.	=	inches
K	=	thermal conductivity
L	=	paint layer thickness
M_∞, *MINF*	=	freestream Mach number

* Graduate Research Assistant, University of Maryland, College Park, MD; inna.kurits@arnold.af.mil
† Professor, Department of Aerospace Engineering, University of Maryland, College Park, MD; mjlewis@umd.edu
‡ Principal, LeaTech LLC, Frederick, MD; mphamner@leatechllc.com
§ Project Engineer, Aerospace Testing Alliance, AEDC White Oak, Silver Spring, MD; joe.norris@arnold.af.mil

mil	=	1 thousandth of an inch
μm	=	micron
ms	=	millisecond
nm	=	nanometer
psia	=	pounds per square inch absolute
P_∞, *PINF*	=	freestream pressure, psia
qdot, q"	=	heat transfer rate
Re	=	Reynolds number
s	=	seconds
St	=	Stanton number, $St = \frac{qdot}{\rho u\left(H_o - C_p T_w\right)}$
surf	=	surface
t	=	time
T	=	temperature
TSP	=	temperature sensitive paint
T_{st}	=	steel temperature
T_{tsp}	=	temperature sensitive coating temperature
T_w	=	wall temperature
u	=	freestream velocity
W	=	Watts
α	=	thermal diffusivity
ρ	=	freestream density
Δx	=	node size through the model wall in the numerical model

I. Introduction

Currently, the evaluation of heat flux at AEDC Hypervelocity Wind Tunnel 9 involves acquisition of surface temperature measurements using thermocouples, i.e. a discrete measurement. At Tunnel 9, these measurements are typically made simultaneously on a single large stainless steel model designed to also acquire force and moment and surface pressure data. Once surface temperatures have been measured, a simple 1-D numerical heat transfer conduction model is used to determine the convective heat flux at the discrete locations of the thermocouples. Unfortunately, most complex flow phenomena cannot be captured adequately using point measurements. Examples of such phenomena include boundary layer transition, flow separation, and shock/boundary layer interactions. In addition, some scale models may be hard or impossible to instrument with thermocouples in areas such as sharp leading edges and control surfaces. Moreover, the cost and time consuming nature of installing discrete instrumentation must be considered in test planning. Hence, the advantages of potentially lower cost and increased instrumentation density of a global technique are desired.

Previous collaborative efforts between Tunnel 9, LeaTech LLC, and the University of Maryland resulted in the development of an intensity-based temperature sensitive paint (TSP) system capable of surviving in the harsh environment of the facility and acquiring high resolution temperature maps of a complex three-dimensional surface. This system and experimental results from its use have previously been reported in **Ref. 2.**

In order to develop the capability to calculate heat flux from TSP, a model of the NASA Crew Exploratory Vehicle (CEV) was tested at Tunnel 9. A temperature sensitive coating of the same formulation used in previous tests at Tunnel 9 was applied to the model. In support of this test, the illumination system development begun in **Ref. 2** was completed and a camera system that met estimated requirements to measure emission from the TSP at sufficient sample rates and resolution requirements was identified. The improved TSP system enabled acquisition of multiple high resolution images during run times on the order of 0.5-1.5 seconds experienced in the test program. This paper describes both the data reduction methodology developed to compute the heat flux using this system and some of the preliminary results.

A. Tunnel 9 Facility Description

Tunnel 9 is a unique blowdown facility that utilizes pure nitrogen as the working fluid and currently operates at Mach numbers of 7, 8, 10, and 14. An operational envelope showing Reynolds number equivalent altitudes versus Mach number for Tunnel 9 operating conditions is presented in **Fig. 1**. The unit Reynolds number range for the facility is from 0.05×10^6 /ft (useful for high- altitude/viscous interaction simulation) to 48×10^6 /ft (duplication of flight dynamic pressure). The test section is over 12 ft long and has a diameter of 5 ft, enabling testing of large-scale model configurations that can include simultaneous force and moment, pressure, and heat-transfer instrumentation. The test cell features a model support system which is capable of dynamically pitching large test articles through an angle-of-attack sweep from -5 to +45 deg at rates of up to 60 deg/s during a typical run. The Mach 10 and 14 nozzles are 40 ft in length with a 60-in.-diam exit. The Mach 8 nozzle is 40 ft in length with a 35-in.-diam exit and operates as a free jet when it is mated to the 60-in.-diam test cell. A photo of the Tunnel 9 Mach 10 nozzle and test cell is provided in **Fig. 2**, and a schematic of the entire facility is shown in **Fig. 3**. Note that flow is from left to right in these figures.

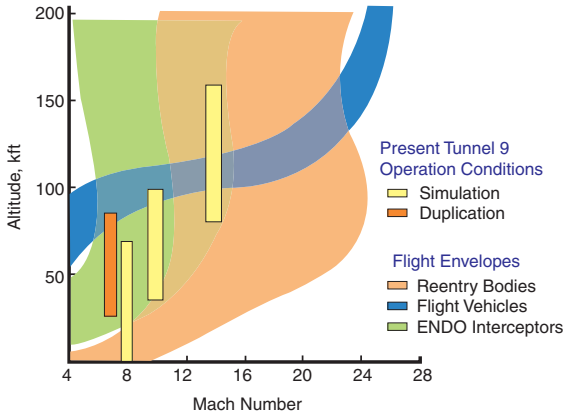

Figure 1. Hypervelocity Wind Tunnel 9 Operational Envelope

Figure 2. AEDC Hypervelocity Wind Tunnel No. 9 Test Cell and Mach 10 Nozzle

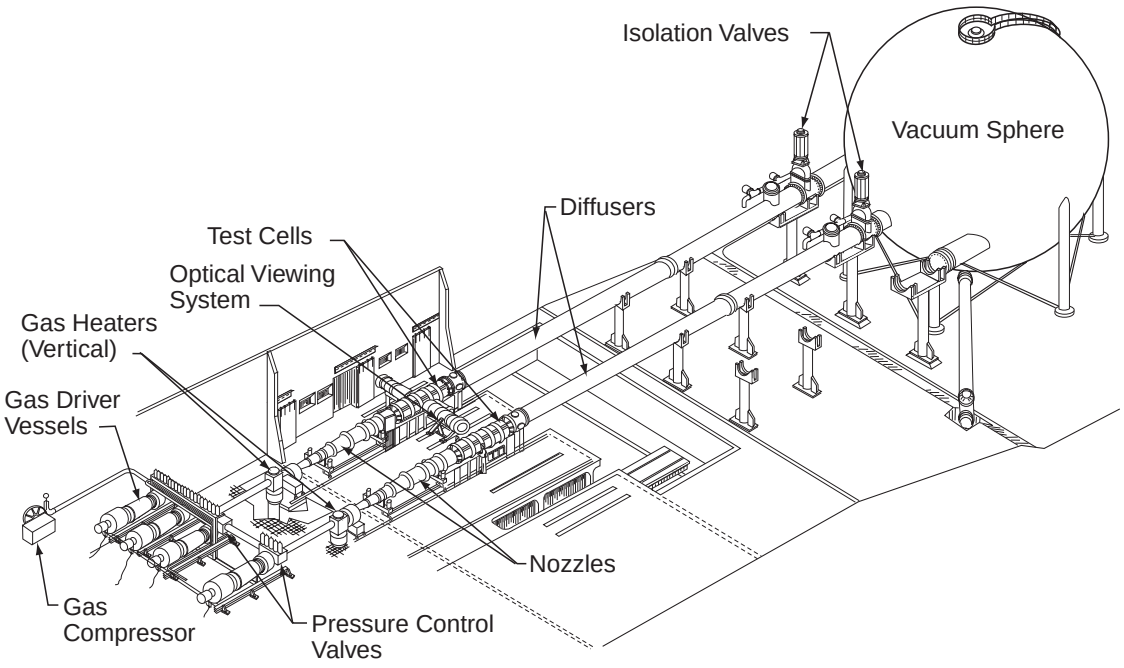

Figure 3. Tunnel 9 Facility Schematic

During a typical run, the vertical heater vessel (left side of Fig. 3) is used to pressurize and heat a fixed volume of nitrogen to a predetermined pressure and temperature defined by the desired freestream conditions. The test cell and vacuum sphere are evacuated to approximately 1 mmHg and are separated from the heater by a pair of metal diaphragms which are located upstream of the throat. When the desired temperature and pressure are reached in the heater, the diaphragms are ruptured. The gas then flows from the top of the heater vessel, expanding through the contoured nozzle into the test section at the desired freestream test conditions. As the hot gas exhausts from the top of the heater, cold nitrogen gas from the pressurized driver vessels enters the heater base. This cold gas drives the hot gas out the top of the heater in a piston-like fashion, thereby maintaining constant conditions in the nozzle supply plenum and the test section during the run. A run is completed once the supply of hot, pressurized gas is exhausted. A more complete description of the Tunnel 9 facility and capabilities can be found in **Ref. 1.**

B. Background

TSP systems have been successfully applied to the study of flows from low subsonic to hypersonic speeds over a wide range of Reynolds numbers including a variety of test conditions, e.g. cryogenic and high-temperature (high enthalpy) conditions. The primary benefit of these types of global mapping systems is the ability to acquire high resolution, quantitative global surface temperature maps for complex three-dimensional models. With an appropriate data reduction algorithm in place, these temperature maps can be converted into heat transfer rates. Convective heat transfer associated with aerodynamic heating of a vehicle traveling at hypersonic speeds is an extremely important factor in the design of hypersonic vehicles. Moreover, a TSP system is potentially less costly and time consuming than the use of discrete measurements currently employed at facilities such as Tunnel 9.

In general, a temperature sensitive coating consists of a binder and photoluminescent (fluorescent or phosphorescent) probes. The photoluminescent probes, or luminophores, are temperature sensitive molecules dispersed within the binder, typically through mixing. The binder is a host matrix, usually a polymer, which forms the coating material. The temperature sensitive molecules undergo a photochemical reaction when excited at the appropriate wavelength and subjected to a change in temperature. The resulting photoluminescence, or emission from the coating, is red-shifted relative to the excitation wavelength and its intensity depends on the temperature. The emitted light intensity is detected by a photodetector, e.g. a photomultiplier tube, photodiode or CCD camera, and is converted into a temperature history by processing the detected intensity using a known calibration curve. For an in-depth description of the photochemical process see **Ref. 3**

There are a few unique challenges associated with developing a TSP system for the use at Tunnel 9. They include high dynamic and thermal loading environment, long run times relative to other hypersonic facilities of similar freestream conditions, and transient heating profiles due to dynamically pitching the model during the run. These conditions impose limitations on the types of models tested at Tunnel 9 and dictate data acquisition and reduction requirements.

As was mentioned earlier, feasibility studies previously conducted at Tunnel 9 demonstrated the survivability of the paint in the extreme conditions of the tunnel as well as the ability to acquire global maps of complex flow phenomena. From these studies the need for improvement in camera detection and illumination systems was identified. A study was conducted to asses various possible illumination sources for their intensity, stability, and operational qualities. A detailed description of this effort is provided in **Ref 2**.

C. Review of Global Heat Transfer Methods for Hypersonic Wind Tunnels

A range of global temperature and heat transfer acquisition techniques have been successfully applied at various hypersonic facilities. In all cases, reducing global temperature data into heat flux is a non-trivial task, and so simplifying assumptions related to specific test conditions usually have to be made to develop a practical data reduction methodology. In other words, the choice of simplifying assumptions which define the heat flux data reduction algorithm depends on the facility and the types of models tested. For instance, a two-color thermographic phosphor technique has been successfully developed and applied to ceramic wind tunnel models by Buck [**Ref 4**] at NASA Langley Research Center at Hampton, VA for several years. The test articles are injected into the flow, which eliminates the need for transient heat transfer modeling. Two factors greatly simplify the heat transfer calculations: 1) step input heating due to model injection and 2) semi-infinite wall assumption, which is reasonable for ceramic models of appropriate thickness.

An example of luminescent paint techniques successfully applied in a hypersonic ground test facility includes the research at the JAXA Hypersonic Shock Tunnel facility by Nakakita et al [**Ref 5**]. The approach taken in this facility in order to simplify the heat transfer data reduction is to utilize a very thin layer of the polymer such that the influence of the typically insulative TSP layer can be neglected. Using typical polymer material properties, the authors estimated that the paint layer can be ignored in the data reduction if it is < 1 μm thick and 2% error in heat transfer rate calculation is acceptable. Then, uniform semi-infinite media assumption can be made in the heat transfer rate calculation, making the data reduction straightforward. Ohmi et al [**Ref 6**] conducted a follow-up experimental study to evaluate this assumption. They tested ceramic models painted with very thin TSP layer (.2-3 μm) and used the same simple 1-D semi-infinite heat conduction model to calculate the heat transfer rate. The TSP layer was ignored in the data reduction and the error associated with this simplification was calculated. They concluded that the paint layer can be ignored in the data reduction if it's < .5 μm, and not 1 μm as previously estimated by Nakakita et al due to the differences between the actual TSP material properties and handbook tabulated polymer material properties. Additionally, the error in calculated heat flux changed non-linearly with the change in paint layer thickness.

Hubner, et al [**Ref 7**] used TSP to measure full-field surface heat transfer rates in short-duration hypersonic flow (run times under 10 ms) at LENS1 shock tunnel at CUBRC. A thick insulating polyurethane layer (100 – 150 μm) was applied between the thin (~5 to 10 μm) active TSP layer and the metal model surface. The heat transfer was calculated assuming adiabatic wall condition, constant step input heat transfer rate and temperature independent thermal conductivity K and thermal diffusivity α.

The initial approach for evaluating heat transfer in Tunnel 9 from global surface temperature measurements follows a somewhat different path than that of previous research. This is due in part to the operation of the facility and the need to use structurally robust stainless steel models that are well suited for force and moment testing in the high Reynolds number environment. The goal is to be able to use the same test articles for TSP tests as are used for force and moment testing in order to reduce complexity and cost due to multiple models for a single test program

In general, the approach at Tunnel 9 was to apply the same transient 1-D finite difference conduction calculations used for reducing coaxial thermocouple data in the standard Tunnel 9 method. However, a second layer was added to the heat transfer model representing the temperature sensitive coating on the model surface. Additional factors that differ from methods outlined above include tunnel start-up time (order of 200 msec) which is non-negligible. Heating profiles during start-up resemble a ramp since the model is not injected into the flow after the facility is started. This means that a step change in heat transfer rate cannot be assumed as in the cases of short duration hypersonic facilities or model

injection into the flow. Furthermore, it is desired to eventually acquire TSP data while dynamically pitching the model during a single run. As a result, the heating input to the model for this application is by nature unsteady since the heating profile is a function of angle of attack. Other factors that must be accounted for in the data reduction include the effects of non-linear thermal conductivity of the paint formulation over the range of temperatures encountered at Tunnel 9 and paint layer thicknesses of approximately 2 mils (~ 50 μm). This thickness is desired in order to increase paint emission so that good signal to noise ratios could be obtained. This is currently considered too thick to be ignored in the heat transfer modeling.

II. Experimental Setup

Similar to TSP systems used in other research facilities, the system developed for use in Tunnel 9 essentially consists of four main components: an illumination system, a detection system, the temperature sensitive coating, and the data processing algorithm. A brief description of each system component is presented below.

The test article was a 7" diameter model of the NASA CEV capsule constructed out of 15-5 stainless steel. The geometry is similar to the Apollo capsules flown in the 1960's. During the Tunnel 9 tests, the pitch angle was fixed at 28° for all TSP runs. The heat shield and portion of the aft cone of the model were coated in temperature sensitive paint.

The physical setup is sketched in **Fig. 4**. Three illumination sources were located on top of the test cell and two on the side to ensure the entire model surface was uniformly illuminated with sufficient radiant intensity to provide for 0.75 to 0.80 percent full well potential of the CCD cameras. Both of the CCD cameras were initially mounted on top of the test cell to provide images of the heat shield (CAM1) and aft-body (CAM2). Later in the program one camera was re-located to the side of the test cell in an attempt to map the flow over the side of the aft cone. The test conditions and camera settings for each run of the NASA CEV test are listed in **Table 1.**

Table 1. Run Matrix

Run #	M_∞	*Unit Re, x106 /ft*	*Binning*		*Frame Rate, Hz*		*Exp Time, s*
			Heat Shield (CAM1)	Aft-cone (CAM2)	Heat Shield (CAM1)	Aft-cone (CAM2)	
1	10	5.00	4 x 4	4 x 4	~ 61 Hz	~ 61 Hz	1.9
2	10	10.00	2 x 2	1 x1	~42 Hz	~ 25 Hz	1.9
3	10	5.00	2 x 2	2 x 2	~42 Hz	~42 Hz	1.9
4	10	10.00	2 x 2	2 x 2	~42 Hz	~42 Hz	1.9
5	10	5.00	2 x 2	2 x 2	~42 Hz	~42 Hz	1.9

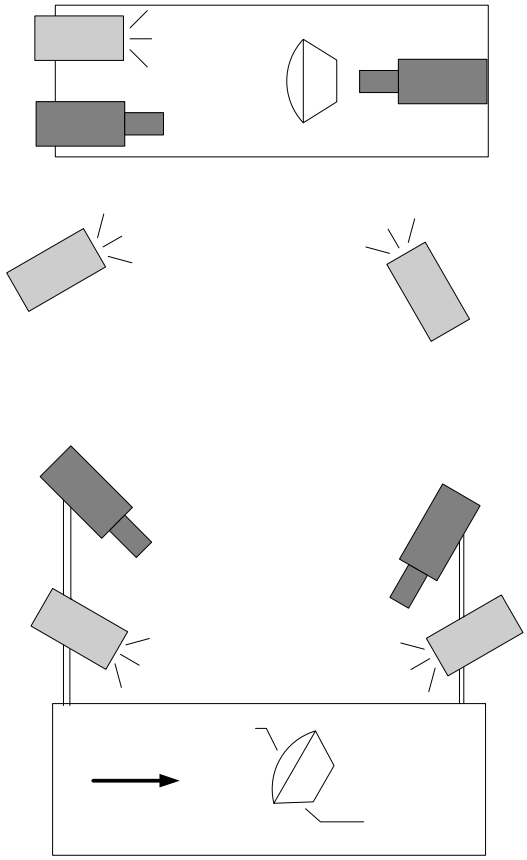

Figure 4: Schematic of the Lights and Cameras for the NASA CEV Test in Tunnel 9

A. System Components and Configuration

Photon Technologies 200W mercury-xenon arc lamps were chosen as optimal illumination source based on their superior stability, intensity and operational qualities assessed in the study described in **Ref. 3**. To provide sufficiently intense and uniform lighting, five lamps were used to illuminate the model. The lights were filtered with a broadband band pass filter centered at 365 nm. The light from each lamp was blocked during periods in which the model did not need to be illuminated to protect the paint from potential photodegradation by the ultraviolet illumination. The output of the lights was monitored by photodiodes to ensure stable output for the duration of each run.

Two PI/Acton PhotonMax 512B cameras were used to enable acquisition of the continuous high quality images required during each run. Per the manufacturer's description, the 512B's are low noise CCD cameras with on-chip multiplication gain via EMCCD (electron multiplication CCD) which multiplies photoelectrons by an impact ionization process prior to readout. The 512B features a 512 x 512 pixel CCD array. It is thought that these cameras should be capable of providing the short exposure times and high frame rates necessary to obtain surface temperature data of suitable quality for calculating heat transfer in Tunnel 9.

The camera exposure time was set to 1.9 sec for all of the runs. A variety of camera settings were tested including 2x2 and 4x4 pixel binning to increase the frame rate. For example, with the full 512x512 CCD array, the effective frame rate for the 512B (including exposure time and readout rate) is only ~ 25 Hz. 2x2 binning resulted in ~ 42 Hz and 4x4 binning in ~ 61 Hz frame rates respectively. The required frame rate for heat transfer calculations will vary depending on test conditions and is currently under study. For example, for a static test (no pitching) with relatively low heating rates, the required frame rate may be as low as 30 Hz.

The temperature sensitive coating used in this test was developed and applied to the test article by LeaTech LLC. Application of the TSP to the test articles used in Tunnel 9 consists of a white basecoat and a temperature sensing layer which are both airbrushed onto the stainless steel model. Both layers were kept as thin as possible while still creating a uniform coating. The coating thickness was measured using a magnetic induction probe. One hundred measurements were made on the heat shield and the aft-body to asses the uniformity of the coating for the paint job. The average paint layer thickness was found to be 2.1 mils (~.53 μm) with a standard deviation of 0.15 mil.

The white basecoat is used to create specular reflection of the excitation light through the paint layer and thus increase paint emission intensity only. It is important to note that the basecoat is not used to create an insulating layer as seen in other TSP systems used with metallic wind tunnel models [**Ref 7, 8]**. The formulation used for the NASA CEV test utilizes a Europium complex as the temperature sensitive luminophore. This paint formulation has a broad absorption spectrum (relative to Europium alone) with excitation centered at 365 nm. This formulation's emission is centered at 614 nm **[Ref 3].** Utilization of Europium gives this formulation very good temperature sensitivity, on the order of tenths of a degree Fahrenheit, that when combined with the high temperature polyurethane developed for use in Tunnel 9 easily withstands temperatures up to 360 F, which is well over the temperature range encountered during this test. Incidentally, there is no uncertainty associated with the paint acting as a pressure sensor via oxygen quenching since the facility uses nitrogen as the working fluid.

Due to the challenging freestream environment in Tunnel 9 at Mach 10 high Reynolds number conditions, the paint had to be reapplied to the test article after the 4th run due to damage to the coating from small particle impacts. The paint was applied over several coaxial thermocouples that were included in the model in order to measure heat transfer via traditional means during the non-TSP runs of another part of the test program. However, a few thermocouples were left unpainted on the heat shield for comparison with symmetrically located painted thermocouples. The locations of painted and unpainted thermocouples are indicated in **Fig. 5.** Black circles were added to the left side of the picture to indicate the painted thermocouples' locations. The black dots on the surface of the paint are the registration marks used to align the images in the image processing software.

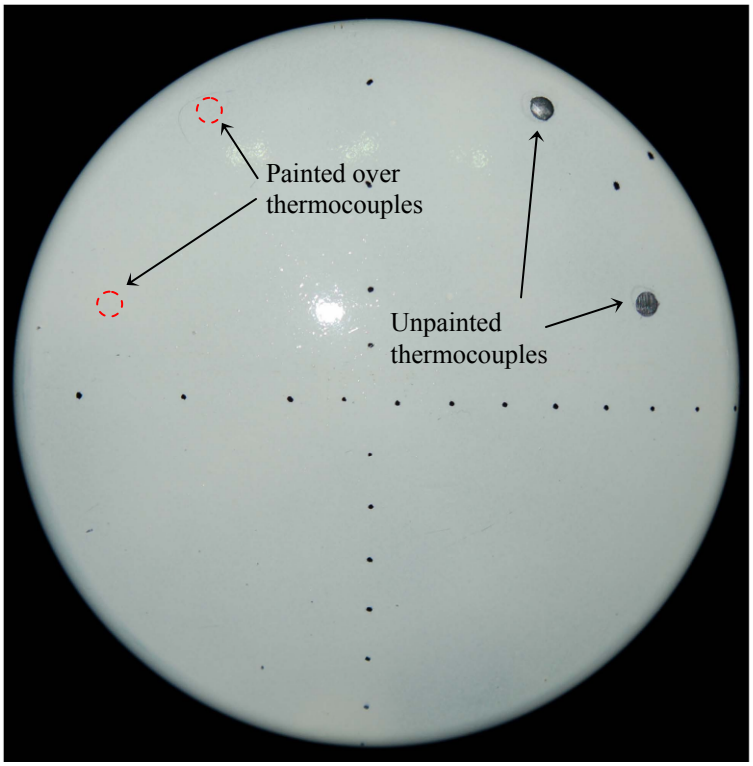

Figure 5: Heat Shield of the CEV model painted with temperature sensitive coating

III. Methodology for the Evaluation of Heat Transfer

In general, the algorithm used to calculate the heat flux from TSP data at Tunnel 9 is based on the same analysis applied to reducing coaxial thermocouple temperature data into heat transfer and is driven by the transient nature of the facility. In essence, a time history of the surface temperature is applied as the boundary condition in a transient 1-D heat transfer conduction model. An example of the temperature history used as the input to the algorithm is shown in **Figure 9**. This model employs a second order Euler-explicit finite difference approximation method to solve transient 1-D heat equation to obtain a one-dimensional temperature distribution at nodes at varying depths through a steel model wall of finite thickness at each time step of the algorithm. The local convective heat transfer rate is calculated based on Fourier's Law using a second order derivative approximation of the temperature profile at the model's surface. At the beginning of the run (initial condition) the model is assumed to be at a uniform initial temperature. Zero heat transfer at the back wall is the remaining boundary condition required to solve the equation numerically. The calculated heat flux uncertainty from coaxial thermocouple data using this approach is ±6%. A detailed description of the coaxial thermocouple data reduction methods used at Tunnel 9 can be found in **Ref. 9.**

To develop an analogous data reduction methodology for evaluating heat transfer using TSP data, a second layer comprising the temperature sensitive coating was added to the 1-D heat transfer model. In reality, the temperature sensitive coating consists of two layers: the basecoat and the active layer. However, the two layers can be treated as one in the data reduction algorithm since they are made of the same host matrix material.

The numerical model is schematically represented in **Fig. 6**. In this case the TSP data becomes the input boundary condition (T_1) at the surface of the model. Then, the heat flux balance at the interface between the two materials (TSP and the model wall material) is enforced using the Fourier's law of conduction (1). One additional assumption is made to simplify the algorithm: the temperature gradient through the paint layer is assumed to be linear. This allows for a very simple discretization of the heat flux balance equation at the interface of the two materials (2).

$$q'' = -K(\partial T/\partial x) \qquad (1)$$

$$K_1 \cdot \frac{T_1 - T_2}{L} = K_2 \cdot \frac{T_2 - T_3}{\Delta x} \qquad (2)$$

Moreover, this assumption eliminates the need for knowledge of the overall thermal diffusivity of the temperature sensitive coating. However, thermal conductivity K of the coating material still needs to be known. Currently, lab measurements of K are being conducted. In the interim, a method for estimating K using thermocouple data available from the NASA CEV test is described in Appendix A of the paper.

Subsequently, the temperature history at nodes through the metal model wall and the local heat transfer at the surface are found using the same numerical method as described above for coaxial thermocouples. 1-D transient heat equation (3) is solved numerically using second order Euler-explicit finite difference approximation (4). Once the temperature distribution through the model wall is known, Fourier's Law of Conduction (5) is applied at the surface of the model to calculate convective heat transfer using second order derivative approximation of the temperature profile at the model's surface (6).

$$\partial T/\partial t = \alpha(\partial^2 T/\partial x^2) \qquad (3)$$

$$\frac{T_{i+1,j} - T_{i,j}}{\Delta t} = \alpha_2 \cdot \left(\frac{T_{i,j+1} - 2T_{i,j} + T_{i,j-1}}{\Delta x^2} \right) \qquad (4)$$

$$\alpha_2 = \frac{K_2}{\rho_2 \cdot C_{p2}}$$

$$q'' = -K(\partial T/\partial x)_{surf} \qquad (5)$$

$$q'' = \frac{-K_1}{L} \cdot \left[-3 \cdot T_{i+1,1} + 4 \cdot \left[\frac{1}{2} \cdot \left(T_{i+1,1} + T_{i+1,2} \right) \right] - T_{i+1,2} \right] \qquad (6)$$

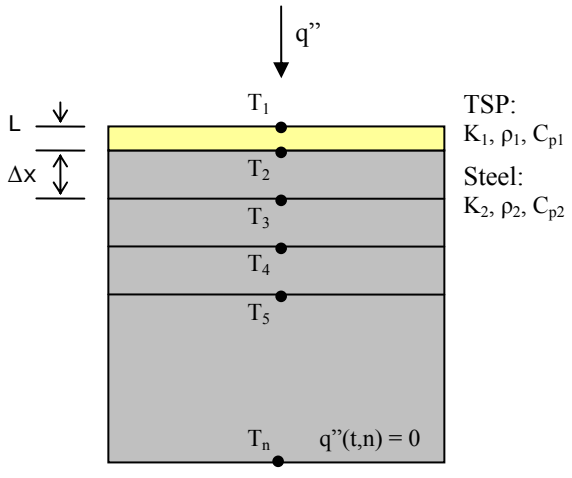

Fig.6: Schematic Representation of the Numerical Model

The linear temperature gradient through the paint layer assumption is justified via an analysis performed by modeling the problem in ANSYS in 1-D. ANSYS is a commercially available powerful finite element modeling tool for structural and thermal analysis. It was used extensively throughout the modeling process as additional means for data reduction algorithm development and validation. The ANSYS simulation was constructed to closely represent the actual test article and test conditions: .375" thick stainless steel model wall (with 200 nodes) painted with .002" thick paint layer (with 6 nodes). A .002 s time step was used to meet the convergence criteria. The actual heating profile experienced during the TSP test and representative thermal properties for the temperature sensitive coating were used. The results are depicted in **Fig. 7.** The location corresponding to x=0 represents the interface between the steel model wall and the temperature sensitive coating, and x = .002 represents the surface of the coating exposed to the flow. From this simulation, it appears that the temperature gradient is linear at lower temperatures, as would occur in the beginning of a run, and can be closely approximated as linear at higher temperatures.

This methodology for evaluating heat transfer offers a simple way of calculating convective heat transfer from TSP data in transient situations where heat transfer can be considered one-dimensional, the temperature sensitive coating is too thick to be ignored, and material properties of the coating, such as the thermal conductivity and thermal diffusivity are functions of temperature. While one-dimensional heat conduction model may seem limiting, it can be applied to many practical geometries tested at Tunnel 9 and other hypersonic facilities. In fact, the heat transfer models used in Ref. 4 – 8 all assume 1-D heat conduction through the model wall. Nevertheless, a technique for solving more complex 2- and 3-D conduction problems is currently being developed.

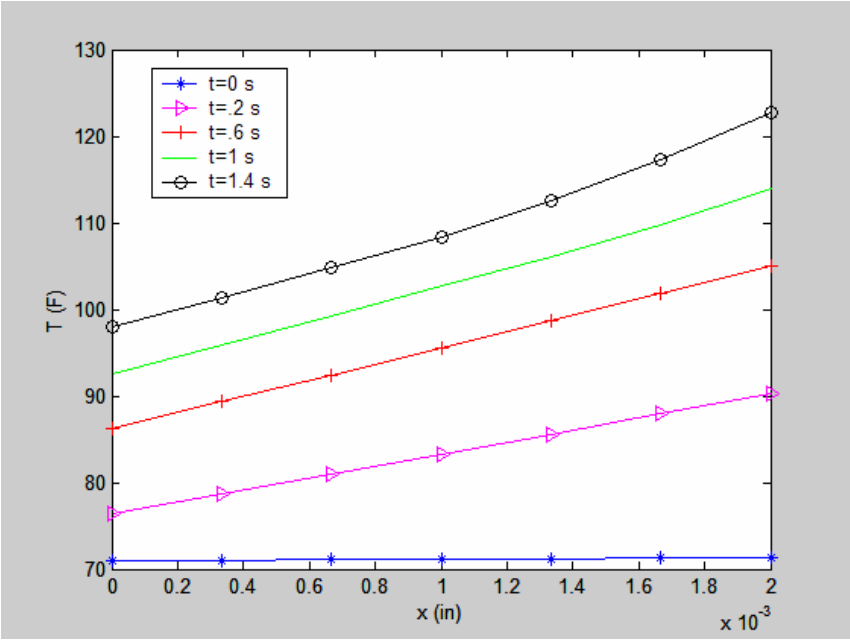

Fig.7: ANSYS simulation of temperature gradient through the temperature sensitive coating

IV. Preliminary Results and Discussion

A. Processing of TSP images

Reference and wind-on (run) images for surface temperature data are acquired using PI/Acton's Winview32 software. Appropriate pre- and post-run images are acquired and archived. Reference and run raw image data is mapped, ratioed, and calibrated using Greenboot software. Surface temperature data is output globally from Greenboot and interrogated using Matlab. All of the heat transfer modeling and data reduction was done using ANSYS and Matlab software packages.

Figure 8 illustrates the time history of ratioed intensity, which is inversely proportional to paint surface temperature, acquired using the TSP system at a location coincident with a thermocouple installed

on the CEV test article. The curvefit of the ratioed intensity history, shown as the black line in Fig. 8, was used as an input to the heat transfer data reduction algorithm to obtain local heat flux. The scattered data points in the beginning of the run (before the "good flow" period) are not representative of the actual paint emission during the startup. The extreme drop in recorded intensity is due to the condensation cloud passing through the test section and obstructing the view of the camera. The missing data in the beginning of the run was inferred from the thermocouple data underneath the paint at this location.

Figure 9 illustrates the time history of TSP image acquisition compared with data acquisition from thermocouples. The red line represents the surface temperature rise recorded by the thermocouple. Each grey bar corresponds to a TSP image acquired during the run, where the width of the bar represents the camera exposure time and the spacing between the bars represents the camera frame rate. It can be seen that the temperature change during each exposure is insignificant, so it is reasonable to assume that the temperature captured by each frame is an instantaneous value at the time of the frame. It is also evident that the ~ 42 Hz frame rate is high enough to resolve the heating rate encountered during this test.

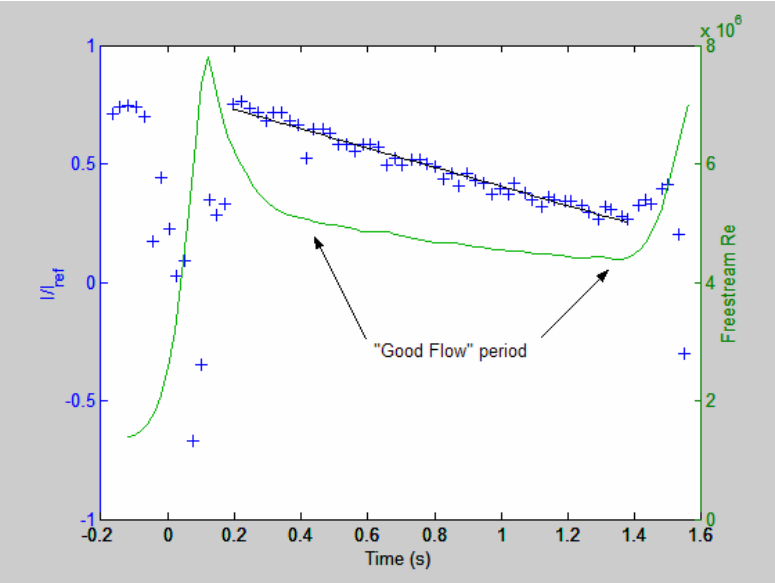

Figure 8: TSP Ratioed Intensity Data at a location corresponding to a painted thermocouple and Freestream Reynolds Number for Run 3

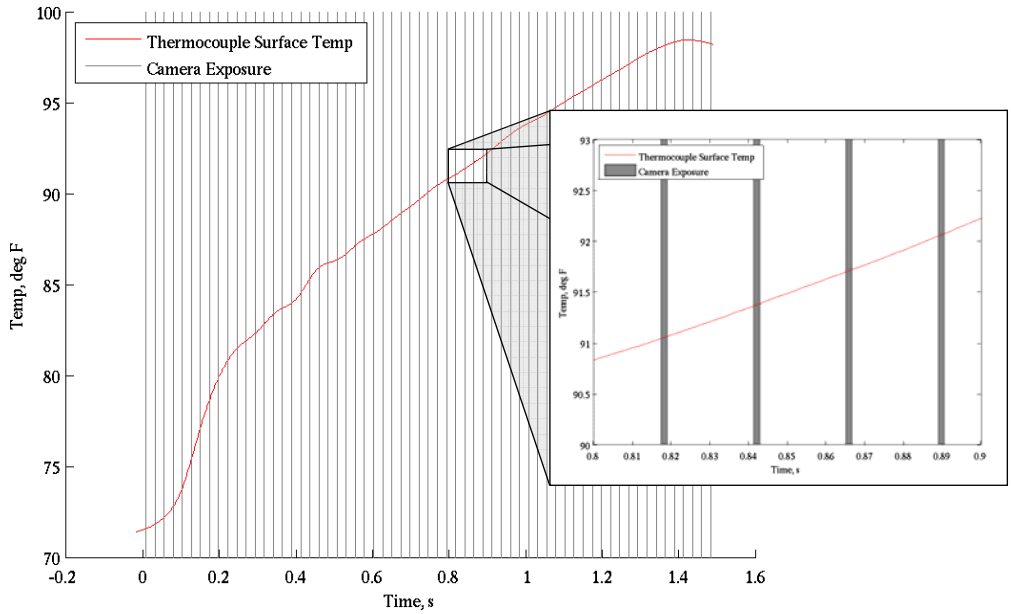

Figure 9: Time History of TSP Image Acquisition for Run 3

B. Global Temperature Evolution

This paper is not intended to summarize the results of each run of the program. Instead, the goal is to present the data reduction methodology. Therefore, results from run 5 will be presented in the following sections. Sequences of high-quality images of the heat shield and the aft-cone that show the evolution of the heating profile in time were acquired during each run. Images of the heat shield from Run 5 are shown here (**Fig. 10**) in order to demonstrate the capability of the composite Tunnel 9 TSP system during the good flow period. For each image, the time in which it was acquired is shown in the figure. It is significant to remind the reader that these images are acquired over a very short exposure time and relatively high frame rate given the 14-bit A/D converter and yet the quality is excellent. This is attributed to the high quantum efficiency of the paint and the high intensity level of the illumination system. As expected, the overall temperature of the model surface shows an increase during the run due to aerodynamic heating.

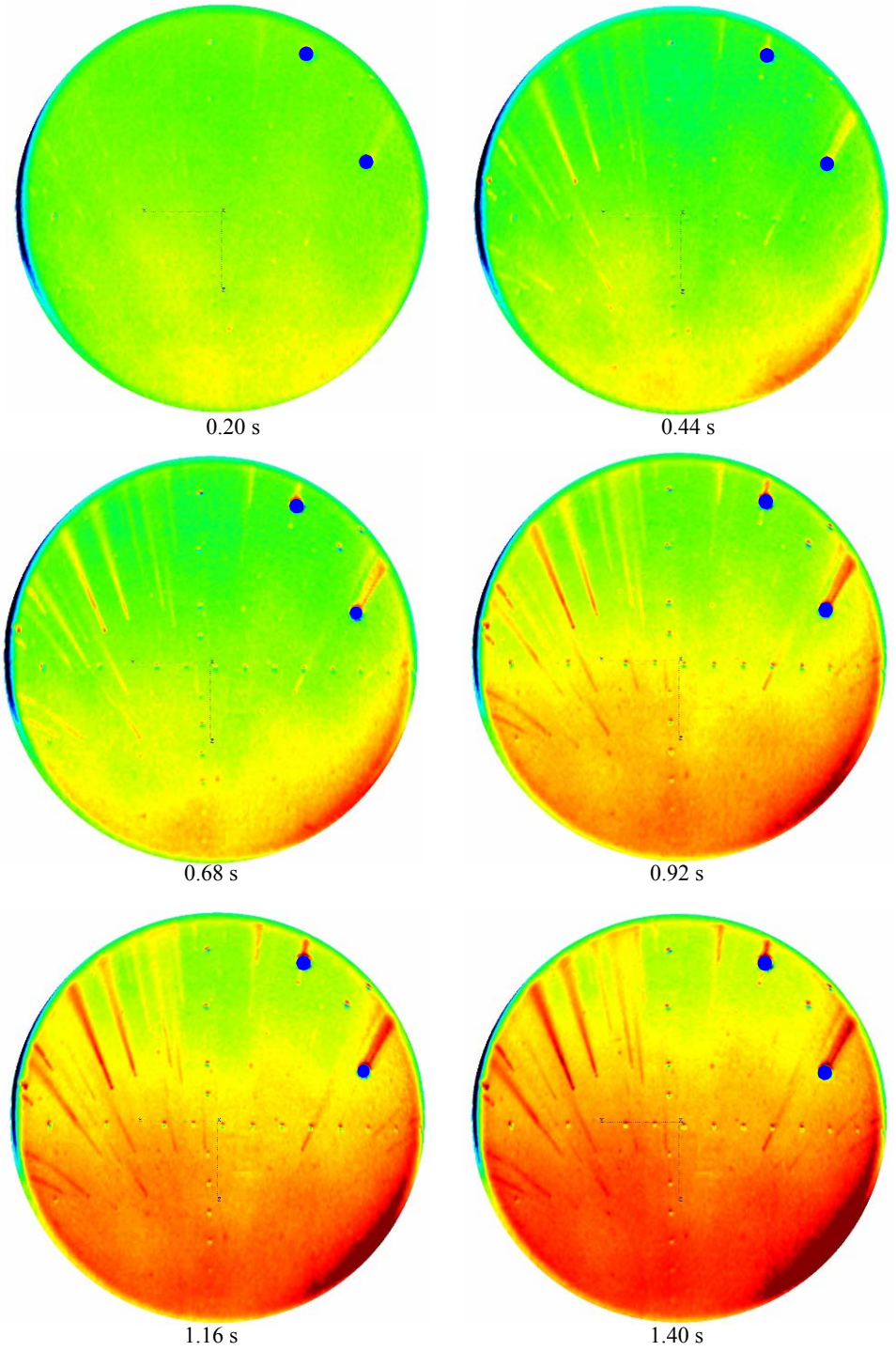

Figure 10: CEV Heat Shield; Mapped, Ratioed, TSP Images during Run 5, Mach 10, Re = 5.0 x 10^6 /ft

The dark blue color on the right hand side of the images is an area out of the field of view of the camera so no TSP data is available. The two unpainted thermocouples in the top right quadrant of the heat shield are also 'blue' indicating that no TSP data are available in those locations. The deepest red color appearing in the lower right corner of the heat shield in some of the images does not represent aerodynamic heating and is due to overlapping of the illumination from two light sources on the model surface which saturates the CCD array. The streaks appearing in some of the images resulted from increased local heating induced by particles impacting the model surface and creating streaks of turbulence during the run.

The curvefit of the time-history of ratioed intensity at the location of a painted thermocouple shown in Fig. 8 was used to estimate the thermal conductivity of the paint as described in Appendix A and also as the input boundary condition to the heat transfer algorithm as described in the Methodology section of the paper. The convective heat flux calculated in this way and non-dimensionalized as Stanton number was compared against the values calculated from unpainted thermocouple data symmetrically located on the model. The Stanton numbers normalized by the stagnation point values are shown in **Fig. 11**. The Stanton number plot only shows the "good flow" period of the test run, which is of primary interest. The Stanton number is constant during the "good flow" period of the run since the model is at a constant angle of attack throughout the run. The red line represents the normalized Stanton number calculated from thermocouple data using the standard data reduction technique, and the green line represents the corresponding values calculated using the proposed algorithm for TSP data reduction. The values are expected to be close since the thermocouple data was used in the thermal conductivity estimation as described in Appendix A, and hence was part of the "calibration" process. However, the ± 3.5 % agreement between the two curves does validate the overall numerical algorithm used for heat flux calculation. To further validate the methodology, the analysis must be applied at other points where no thermocouple data is available. The analysis is being conducted at the time of this paper's publication.

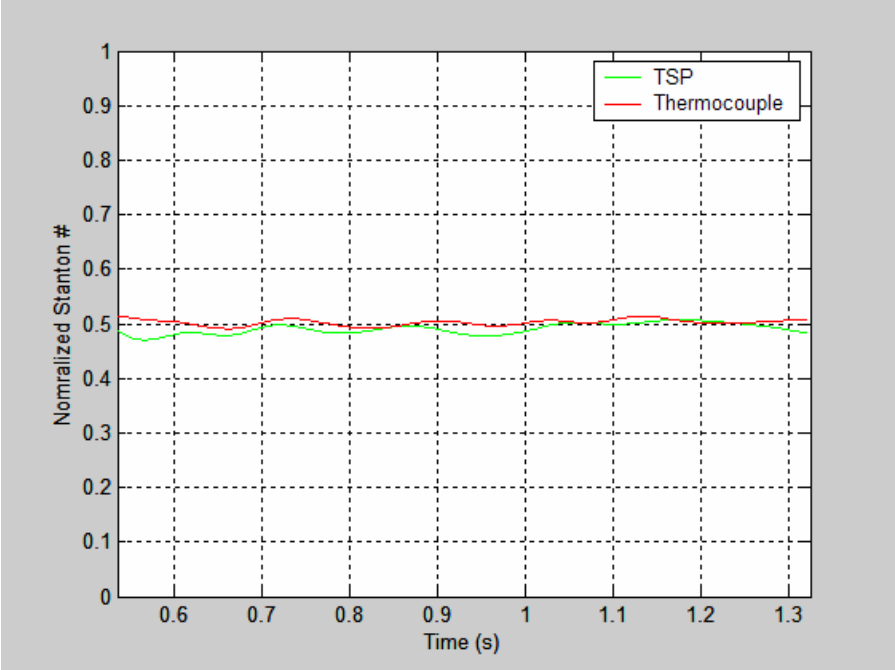

Fig.11: Normalized Stanton Numbers calculated from Thermocouple and TSP data

V. Summary

Tests of a NASA CEV model at AEDC Hypervelocity Wind Tunnel 9 were used as part of the development of a methodology for using TSP surface temperature data to evaluate heat transfer. To achieve this, the CEV model was painted with TSP and multiple high-quality images were acquired during five runs in the test program. TSP images acquired have been successfully converted into global temperature maps. The sequences of consecutive images have been used to demonstrate the ability to map out the temporal evolution of the global surface temperature profile on both the heat shield and the aft-cone portions of the model. A data reduction methodology to calculate convective heat transfer on the surface of the model for a transient 1-D conduction case where presence of the TSP layer cannot be ignored has been studied. A temperature dependent value for thermal conductivity of the temperature sensitive coating was estimated using TSP and thermocouple data. The estimated value of thermal conductivity was then used to calculate the heat flux from the TSP surface temperature data at one point to validate the overall

computational scheme. The heat flux calculated from TSP data correlates well with the value obtained from thermocouple data.

Further development of this methodology includes direct determination of material properties of the temperature sensitive coating and the computational algorithms to reduce TSP data over the entire surface of a test article. In addition, an estimate of the system's noise and resulting uncertainty in calculated convective heat flux will be made. An approach to dealing with 2-D and 3-D heat transfer problems is also being developed.

Acknowledgements

The authors would like to acknowledge the financial support of NASA (Randy Lillard of JSC and Tom Horvath of LaRC) and the dedication of the Tunnel 9 team before, during and after this effort. Without their ongoing support this work would not have been possible. As always, the assistance and technical support of Marvin Sellers of AEDC is graciously appreciated.

References

[1]Ragsdale, W. C. and Boyd, C. F., *Hypervelocity Wind Tunnel 9 Facility Handbook, Third Edition*, NAVSWC TR 91-616, July 1993, Silver Spring, MD.

[2]Norris, J., Hamner, M., Lafferty, J., Smith, N., Lewis, M., "Adapting Temperature-Sensitive Paint Technology for use in AEDC Hypervelocity Wind Tunnel 9," AIAA Paper 2004-2191, 24th AIAA Aerodynamic Measurement Technology and Ground Testing Conference, Portland, OR, 28 June – 1 July, 2004.

[3]Rabek, J. F., "Mechanisms of Photophysical Processes and Photochemical Reactions in Polymers," Wiley, New York, 1987. Chap. 1.

[4]Buck, G., "Surface Temperature/Heat Transfer Measurement Using A Quantitative Phosphor Thermography System," AIAA-91-0064, 29th Aerospace Science Meeting, Reno, NV, January 1991.

[5]Nakakita, K., Osafune, T., Asai, K., "Global Heat Transfer Measurement in Hypersonic Shock Tunnel Using Temperature Sensitive Paint," AIAA Paper 2003-743, 41st Aerospace Sciences Meeting & Exhibit, Reno, NV, January 2003.

[6]Ohmi, S., Nagai, H., Asai, K., "Effect of TSP Layer Thickness on Global Heat Transfer Measurement in Hypersonic Flow," AIAA Paper 2006-1048, 44th Aerospace Sciences Meeting & Exhibit, Reno, NV, January 2006.

[7]Hubner, J., Carroll, B., Schanze, K., "Heat Transfer Measurements in Hypersonic Flow Using Luminescent Coating Techniques," AIAA 2002-0741, 40th AIAA Aerospace Sciences Meeting & Exhibit, Reno, NV, January 2002.

[8]Matsumura, S., "Streamwise Vortex Instability and Hypersonic Boundary-Layer Transition on the Hyper-2000," Master's Thesis, School of Aeronautics and Astronautics, Purdue University, West Lafayette, IN, Dec 2003.

[9]Boyd, C. F., Howell, A., "Numerical Investigation of One-Dimensional Heat-Flux Calculations," Dahlgren Division, Naval Surface Warfare Center, Silver Spring, MD, 25 October, 1994.

[10]Paul, K. C., Pal, A. K., Ghosh, A. K., Chakraborty, N. R., "Thermal Measurements of Coating Films Used for Surface Insulation and Protection," Surface Coatings International Part B: Coatings Transactions, Vol. 87, B2, 71-148, June 2004.

Appendix A - Estimation of the Temperature Sensitive Coating's Thermal Conductivity

The data reduction algorithm outlined above requires knowledge of the temperature sensitive coating's thickness as well as its thermal conductivity, K. To determine the effect of the coating's thickness and thermal conductivity on computational results, a sensitivity analysis was performed using the same ANSYS 1-D transient heat conduction model described above to assess the effect of perturbations in thermal conductivity and paint layer thickness on the calculated heat transfer rate. From this simple sensitivity analysis it was found, for example, that underestimating the thickness of the temperature sensitive coating by 50% resulted in approximately a 35% error in calculation of heat transfer from the

paint, while overestimating the thickness by 50% resulted in approximately a 21% error. This nonlinear change in the calculated heat flux error with changes in paint layer thickness is consistent with experimental results presented by Ohmi et al in **Ref. 6.** As mentioned previously, the thickness of the paint was measured on the actual model itself. Based on the standard deviation of 0.15 mils for the 2.0 mil thickness, the paints thickness is known within 7.5%. This gives an estimated error in calculated heat transfer rate based only on uncertainty of the paint thickness of about 4%.

Moreover, the study showed that the error in calculated heat flux increased linearly with increasing error in thermal conductivity, K: ±10% error in K resulted in approximately ±5% change in calculated heat flux, and similarly, ±20% error in K resulted in approximately ±10 % change in calculated heat flux. The above analysis indicates that the thickness of the coating cannot be ignored and the thermal conductivity of the coating applied to a test article in Tunnel 9 cannot be assumed constant for heat transfer calculations. While the paint layer thickness can be measured directly, the measurement of thermal conductivity of a polymer-based coating is non-trivial.

A method was developed to estimate the value of thermal conductivity of the coating as a function of temperature using thermocouple and TSP data available from the test. To make an estimate of the thermal conductivity of the temperature sensitive coating used in the test, temperature data from two pairs of standard coaxial thermocouples on the heat shield of the CEV model located symmetrically about the vertical plane on the left and right hand sides of the model were used as follows. During the TSP runs, two thermocouples on the right hand side of the model were left unpainted, while their symmetric counterparts were painted along with the rest of the model as shown in **Fig. 5**. A pair of these symmetrically located thermocouples was modeled as is graphically represented in **Fig 12**., where T_{1_tsp} is the TSP temperature data over painted thermocouple, T_{2_tsp} is the painted thermocouple data, T_{1_st} is the unpainted thermocouple data, T_{2_st} is calculated using 1-D heat conduction finite difference model, $K_1(T)$ is the thermal conductivity of TSP, $K_2(T)$ is the thermal conductivity of the model material (stainless steel), St is the non-dimensionalized heat input, Δx is the node size through model wall, and L is the paint layer thickness. The Stanton number was equal at the two symmetrically located points on the model, which corresponded to the painted and unpainted thermocouples (1). A linear temperature profile through the paint layer was assumed once again, which allowed to discretize Fourier's Law of conduction at the surface (2) in the same way as in the heat transfer data reduction model (3,4).

$$St_1 = St_2 \tag{1}$$

$$qdot = -K\,(dT/dx)_{surf} \tag{2}$$

$$qdot_{tsp} = K_1 \frac{T_{1tsp} - T_{2tsp}}{L} \tag{3}$$

$$qdot_{st} = K_2 \cdot \frac{T_{1\cdot st} - T_{2\cdot st}}{\Delta x} \tag{4}$$

From Stanton number definition:

$$St = \frac{qdot}{\rho u\left(H_o - C_p T_w\right)} \quad \text{and} \quad \text{Eqn. 1}$$

$$\frac{qdot_{st}}{\rho u\left(H_o - C_p T_{1st}\right)} = \frac{qdot_{tsp}}{\rho u\left(H_o - C_p T_{1tsp}\right)} \tag{5}$$

Substituting 3 and 4 into 5 and solving for K_1 yields:

$$K_1 = K_2 \frac{L}{\Delta x}\left(\frac{T_{1\cdot st} - T_{2\cdot st}}{T_{1tsp} - T_{2tsp}}\right)\left(\frac{H_o - C_p T_{1tsp}}{H_o - C_p T_{1st}}\right) \tag{6}$$

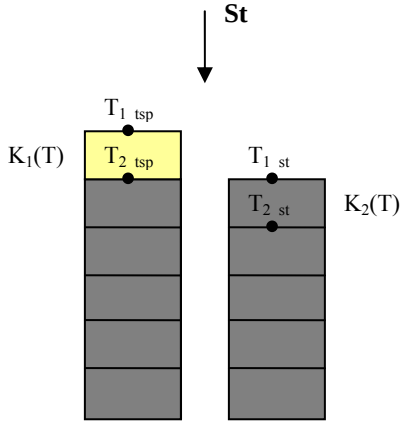

Figure 12: Graphical representation of two symmetrically located thermocouples. One is painted with TSP and the other is unpainted.

The resulting $K_1(T)$ estimate agrees reasonably well with the thermal conductivity of polyurethane based synthetic enamel paint measured by Paul et al [**Ref 10**] as shown in **Fig. 13.** Note that the current estimate for thermal conductivity extends the temperature range to lower temperatures than those measured by Paul et al. It is observed that there is a strong gradient in K as a function of temperature at these lower

temperatures. This again points to the fact that K cannot be assumed constant for heat transfer calculations at Tunnel 9 since the models are initially at room temperature and only reach higher temperatures corresponding to the more "level" part of the curve towards the end of the run.

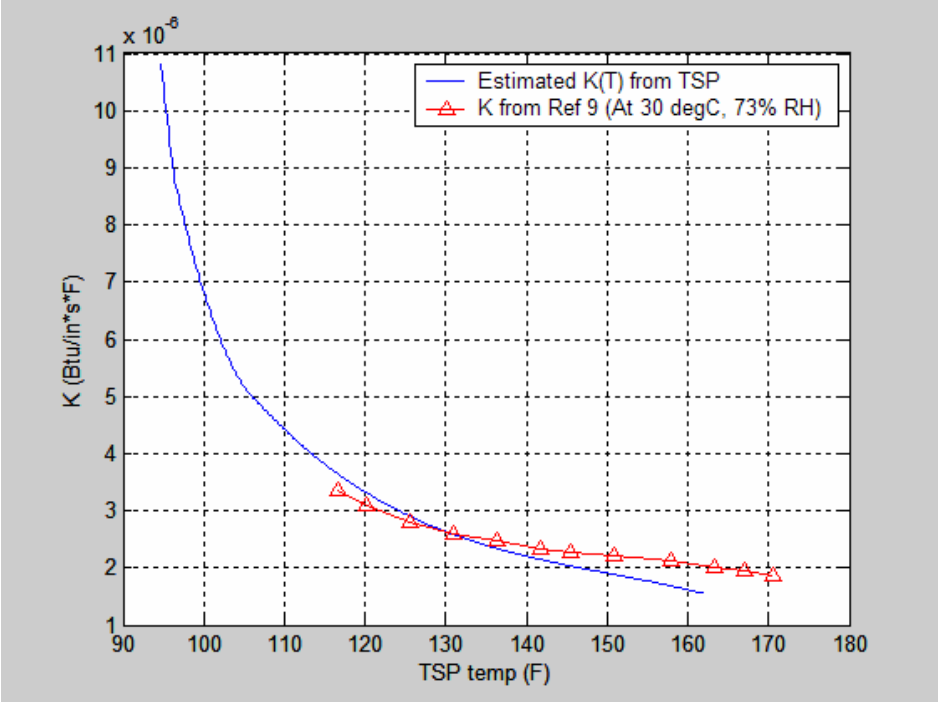

Fig.13: K comparison for the two polyurethane based paints

[1]Ragsdale, W. C. and Boyd, C. F., *Hypervelocity Wind Tunnel 9 Facility Handbook, Third Edition*, NAVSWC TR 91-616, July 1993, Silver Spring, MD.